



HHS Public Access

Author manuscript

Neuroimage. Author manuscript; available in PMC 2017 January 15.

Published in final edited form as:

Neuroimage. 2016 January 15; 125: 267–279. doi:10.1016/j.neuroimage.2015.10.010.

Trajectories of cortical thickness maturation in normal brain development – The importance of quality control procedures

Simon Ducharme^{1,2}, Matthew D. Albaugh³, Tuong-Vi Nguyen^{2,4}, James J. Hudziak³, J. M. Mateos-Pérez¹, Aurelie Labbe^{5,6}, Alan C. Evans¹, and Sherif Karama^{1,5} for the Brain Development Cooperative Group

Matthew D. Albaugh: matthew.albaugh@med.uvm.edu; Tuong-Vi Nguyen: tuong.v.nguyen@mcgill.ca; James J. Hudziak: james.hudziak@med.uvm.edu; J. M. Mateos-Pérez: jose.mateosperez@mcgill.ca; Aurelie Labbe: aurelie.labbe@mcgill.ca; Alan C. Evans: alan.evans@mcgill.ca

¹Montreal Neurological Institute, McConnell Brain Imaging Centre, McGill University, 3801 University Street, Montreal, QC (Canada) H3A 2B4

²McGill University Health Centre, Department of Psychiatry, McGill University, 1025 Pine Avenue West, Montreal, QC (Canada) H3A 1A1

³Vermont Centre for Children, Youth and Families, Fletcher Allen Pediatric Psychiatry, University of Vermont, 1 South Prospect Street, Arnold, Level 3, Burlington, VT 05401

⁴McGill University Health Centre, Department of Obstetrics-Gynecology, McGill University, Montreal, QC (Canada) H3A 1A1

⁵Douglas Mental Health University Institute, Department of Psychiatry, McGill University, 6875 Lasalle Boulevard, Verdun, QC (Canada) H4H 1R3

⁶Douglas Mental Health University Institute, Department of Epidemiology, Biostatistics and Occupational Health, McGill University, 6875 Lasalle Boulevard, Verdun, QC (Canada) H4H 1R3

Abstract

Several reports have described cortical thickness (CTh) developmental trajectories, with conflicting results. Some studies have reported inverted-U shape curves with peaks of CTh in late childhood to adolescence, while others suggested predominant monotonic decline after age 6. In this study, we reviewed CTh developmental trajectories in the NIH MRI Study of Normal Brain

Corresponding authors: 1) Simon Ducharme, MD MSc, Montreal Neurological Institute, McConnell Brain Imaging Centre, McGill University, 3801 University Street, Montreal, QC (Canada) H3A 2B4; Phone: 514-398-1911 #1; Fax: 514-398-2745; simon.ducharme@mcgill.ca. 2) Sherif Karama, MD PhD, Montreal Neurological Institute, McConnell Brain Imaging Centre, McGill University, 3801 University Street, Montreal, QC (Canada) H3A 2B4; Douglas Mental Health University Institute, Department of Psychiatry, McGill University, 6875 Lasalle Boulevard, Verdun, QC (Canada) H4H 1R3; Phone 514-761-6131; sherif.karama@mcgill.ca.

Authors do not report conflicts of interest related to this work.

Disclaimer

The views herein do not necessarily represent the official views of the National Institute of Child Health and Human Development, the National Institute on Drug Abuse, the National Institute of Mental Health, the National Institute of Neurological Disorders and Stroke, the National Institutes of Health, the U.S. Department of Health and Human Services, or any other agency of the United States Government.

Publisher's Disclaimer: This is a PDF file of an unedited manuscript that has been accepted for publication. As a service to our customers we are providing this early version of the manuscript. The manuscript will undergo copyediting, typesetting, and review of the resulting proof before it is published in its final citable form. Please note that during the production process errors may be discovered which could affect the content, and all legal disclaimers that apply to the journal pertain.

Development, and in a second step evaluated the impact of post-processing quality control (QC) procedures on identified trajectories. The quality-controlled sample included 384 individual subjects with repeated scanning (1–3 per subject, total scans $n=753$) from 4.9 to 22.3 years of age. The best-fit model (cubic, quadratic, or first-order linear) was identified at each vertex using mixed-effects models. The majority of brain regions showed linear monotonic decline of CTh. There were few areas of cubic trajectories, mostly in bilateral temporo-parietal areas and the right prefrontal cortex, in which CTh peaks were at, or prior to, age 8. When controlling for total brain volume, CTh trajectories were even more uniformly linear. The only sex difference was faster thinning of occipital areas in boys compared to girls. The best-fit model for whole brain mean thickness was a monotonic decline of 0.027 mm per year. QC procedures had a significant impact on identified trajectories, with a clear shift toward more complex trajectories when including all scans without QC ($n=954$). Trajectories were almost exclusively linear when using only scans that passed the most stringent QC ($n=598$). The impact of QC probably relates to decreasing the inclusion of scans with CTh underestimation secondary to movement artifacts, which are more common in younger subjects. In summary, our results suggest that CTh follows a simple linear decline in most cortical areas by age 5, and all areas by age 8. This study further supports the crucial importance of implementing post-processing QC in CTh studies of development, aging, and neuropsychiatric disorders.

Keywords

Brain development; cortical thickness; maturation; magnetic resonance imaging; quality control; cortical surface area; cortical volume

1. INTRODUCTION

The human brain undergoes rapid development in utero and during the first few years of life (<http://www.bic.mni.mcgill.ca/~vfonov/obj2/obj2model2.mpg>)¹. Although this process slows down after 4 years of age, significant remodeling of the cortex continues up to the late twenties/early thirties^{2,3}. The advent of longitudinal magnetic resonance imaging (MRI) scanning of the developing brain has allowed for a better understanding of typical cortical development. Understanding cortical developmental trajectories of healthy children and adolescents is of crucial importance given the demonstrated impact of cortical maturation on intellectual capacities, behavior, and pediatric neuropsychiatric disorders^{2,4–11}.

Initial MRI studies of brain development used cortical volume as the main morphometric measure. In a landmark study, Giedd et al. (1999) found that cortical volume follows an ‘inverted U’ shape development¹². Gray matter was found to increase in volume in childhood, but started to decline after peaks in adolescence that varied across the different brain areas (age 12 in fronto-parietal, 16 in temporal, 20 in occipital). In addition, average peaks occurred earlier in females^{8,12}. A subsequent detailed study of 13 subjects with repeated scanning over 8 to 10 years revealed that higher-order association areas mature after lower-order somatosensory areas, and that phylogenetically newer areas mature later than older ones¹³.

With the improvement of automated cortical surface measurement, subsequent studies have been able to distinguish cortical thickness (CTh) and cortical surface area (CSA) as two components underlying cortical volume (CV). Major studies in large cohorts have mostly characterized the developmental changes in CTh over time. In a study of 375 typically developing subjects between the ages of 3.5 and 33, Shaw et al. (2008) suggested that CTh of brain regions follow variable trajectories of developmental trajectories based on the complexity of the underlying laminar architecture³. The trajectory was cubic for most of the brain (initial increase, decline in teenage years, then stabilization phase), with some areas (e.g., insular cortex, anterior cingulate cortex) following a quadratic trajectory (initial increase followed by a decline in teenage years), and some areas showing first-order linear decline (e.g., orbito-frontal cortex, subgenual anterior cingulate cortex, medial temporal cortex). Peaks of CTh were attained in primary sensory-motor areas first, followed by secondary association areas, and finally in polymodal association areas. Peaks of CTh occurred earlier than what was reported in older studies (e.g., 10.5 years of age in dorsolateral prefrontal cortex and cingulate cortex). In a later study on 647 typically developing children and young adults (age 3–30), Raznahan et al. (2011) reported a curvilinear ('inverted U') growth pattern of mean CTh¹⁴. Contrary to previous reports, CTh peaks were not sexually dimorphic (8.6 males, 8.4 females)¹⁴. Although CSA trajectories have been less extensively investigated, Raznahan and colleagues (2011) showed a similar curvilinear growth pattern, with later peaks than for CTh (9.7 males, 8.1 females).

In contrast, some studies have not identified 'inverted U' shape or cubic developmental trajectories of gray matter, and casted doubts on the precise age of CTh peaks. A longitudinal study of 45 subjects between the ages of 5 and 11 showed primarily cortical thinning during this age period, except in small parts of the inferior frontal and perisylvian areas¹⁵. Another study of preadolescents (n=126) showed only thinning between 6 and 10 years of age, with minimal differences between males and females¹⁶. In 68 healthy participants from 8 to 30 years of age, Tamnes et al. (2010) reported no increase in CTh after age 8, and regions following quadratic trajectories showed an accelerating decline in adolescence as opposed to a U shaped curve¹⁷. Another sample from the Netherlands also showed almost exclusively linear decline in thickness and gray matter volume between 8 and 30 years of age, with no gender differences in CTh trajectories¹⁸. A study of cortical thickness in twins has reported only thinning between the ages of 9 and 12, in addition to demonstrating a strong increasing genetic influence on mean and local thickness (65% at age 9, 82% at age 12)¹⁹. Finally, in 137 healthy subjects between 6.3 and 29.7 years of age (total 209 scans), Mutlu et al. (2013) did not find evidence of cubic trajectories using a Bayesian information criterion²⁰. There were quadratic trajectories in the frontal and parietal association areas, the temporo-parietal junction, medial frontal areas, and the posterior cingulate/precuneus. However, the large majority of areas showed a first-order linear decline. In summary, although the general assumption is that CTh follows a curvilinear or cubic trajectory, there are inconsistencies across samples, and the age at which CTh peaks remains uncertain.

The NIH MRI Study of Normal Brain Development is a scientific initiative aiming to provide better understanding of normal brain development and brain-behavior relationships²¹. In this study, 431 subjects between 4.6 and 18 years of age were recruited

throughout 6 sites in the USA after a careful assessment to select only typically developing children. A major strength of this study was the population-based sampling method of recruitment with continuous monitoring to ensure socio-demographic representation of the American population²². In an initial cross-sectional report (only the first visit for each subject), total and lobar gray matter volume linearly declined over time (1.11% decline per year), while white matter increased over time (1.54% per year)²³. The only significant sex difference was the previously reported 10% greater total brain volume (TBV) in males compared to females.

In this study, we explored the maturational trajectory of local CTh across the whole brain in the NIH MRI Study of Normal Brain Development. Given the preliminary cross-sectional finding of monotonic linear decrease of gray matter volume in this database²³ and assuming some degree of association between volume and thickness, we expected that if higher order trajectories were present, CTh peaks occur prior to the lower age limit of the studied sample (age 5–6), which is earlier age than peaks reported in past studies that identified inverted-U shape trajectories (age 8.4–10.5)^{3,14}. The impact of factoring TBV as a control variable was also analyzed in order to differentiate absolute morphological changes from relative remodeling in the cortical mantle. We decided to focus on CTh (as opposed to CSA or CV) because variations in this measure have been most frequently associated with cognitive and behavioral phenotypes in children. However, data on trajectories for CSA and CV are provided in an associated Data in Brief article²⁴.

In a second step, we explored the impact of implementing various levels of quality control (QC) on the estimation of CTh trajectories. Given the sensitivity of CTh estimations to very small movement artifacts (some present but hard to notice on native MRI volumes), our group always systematically implements a visual quality control of extracted white and gray matter surfaces to eliminate subjects with probable erroneous measurements. We hypothesize that differences in results of cortical trajectories between research groups could be explained in part by different QC methods. Indeed, Reuter et al (2014) recently demonstrated that movement artifacts can lead to underestimation of CTh.²⁵ By excluding any post-processing MRI with inadequate tissue identification, we ensure that only reliable data are included in statistical analyses. Although QC can decrease sample size and power, this is counterbalanced by a reduction in variance by minimizing the artificially inflated component of the variance due to movement artifacts. This issue is especially important for younger subjects who tend to move more during MRI data acquisition.

2. MATERIAL AND METHODS

2.1 Sampling and Recruitment

Subjects were recruited at 6 pediatric study centers across the USA with a population-based sampling method seeking to minimize selection biases²². There were extensive exclusion criteria including the presence of a current or past Axis I diagnosis established with the Diagnostic Interview for Children and Adolescents (with the exception of simple phobia, social phobia, adjustment disorder, oppositional defiant disorder, enuresis, encopresis, and nicotine dependence), any Child Behavior Checklist syndrome T-score ≥ 70 , family history of major axis I disorder, family history of inherited neurological disorder or mental

retardation due to non-traumatic events, abnormality on neurological examination, gestational age at birth <37 weeks or >42 weeks, and intra-uterine exposure to substances known or highly suspected to alter brain structure or function. A more exhaustive list of inclusion/exclusion criteria is available in Evans et al. (2006) ²¹.

Based on available US Census 2000 data, 431 healthy children from 4 years and 6 months to 18 years and 3 months (age at the first visit) were recruited (Objective 1) with continuous monitoring in order to ensure that the sample was demographically representative on the basis of variables that included age, gender, ethnicity, and socioeconomic status. Informed consent from parents and child assent were obtained for all subjects.

All subjects underwent extensive cognitive, neuropsychological and behavioral testing along with up to three MRI brain scans at two-year intervals. Structural MRI and clinical/behavioral data were consolidated and analyzed within a purpose-built database at the Data Coordinating Center of the Montreal Neurological Institute (MNI), McGill University.

2.2 MRI protocol

Subjects underwent 30–45 minutes of data acquisition (1.5T), with whole brain coverage and multiple contrasts (T1W, T2W and PDW) ²¹. A 3D T1-weighted spoiled gradient recalled echo sequence was selected. The protocol provided 1 mm isotropic data from the entire head, except for subjects scanned on GE scanners for which slice thickness was increased to 1.5 mm due to the limited maximum number of slices. As the priority measure for Objective 1, it was acquired immediately following the localizer scan and, if significant motion artifacts were observed, was immediately repeated. Sagittal acquisition was chosen, being the most efficient way to obtain complete head coverage. For subjects who could not tolerate this optimal procedure, a fallback MR protocol that consisted of shorter 2D acquisitions was used.

Dual contrast, proton density, and T2-weighted (PDW and T2W) acquisitions provided additional information for automated multi-spectral tissue classification/segmentation. An optimized 2D multislice (2 mm) dual echo fast spin echo sequence was used. An oblique axial orientation (parallel to the AC – PC line) was selected. Both American College of Radiology and living phantoms (volunteers repeatedly scanned at each site) were regularly scanned at each site to confirm the inter-site reliability of anatomical measurements ^{21,26,27}.

2.3 Automated Image Processing

All quality-controlled MR images were processed through the CIVET pipeline (version 1.1.11) (<http://wiki.bic.mni.mcgill.ca/index.php/CIVET>) developed at the MNI for fully automated structural image analysis. The main pipeline processing steps include:

1. Linearly registering native (i.e., original) MR images to standardized MNI-Talairach space based on the ICBM152 data set ^{28–30}. This step is implemented in order to account for gross volume differences between subjects.
2. Correct for intensity non-uniformity artifacts using N3 ³¹. These artifacts are introduced by the scanner and need to be removed to minimize biases in estimating gray matter boundaries.

3. Classify the image into white matter, gray matter, cerebrospinal fluid and background using a neural net classifier (INSECT) ³².
4. Fit images with a deformable mesh model to extract 2-dimensional inner (white matter/gray matter interface) and outer (pial) cortical surfaces for each hemisphere with the 3rd edition of CLASP³³. This produces high-resolution hemispheric surfaces with 81,924 polygons^{27,33–35}. This step places 40,962 vertices (i.e., cortical points) on each hemisphere for each subject.
5. Register both cortical surfaces for each hemisphere non-linearly to a high resolution average surface template generated from the ICBM152 data set in order to establish inter-subject correspondence of the cortical points ^{30,35,36}.
6. Apply a reverse of the linear transformation performed on the images of each subject to allow CTh estimations to be made at each cortical point in the native space of the magnetic resonance image. This avoids having estimations biased by the scaling factor introduced by the linear transformations (i.e. step 1) applied to each subject's brain.
7. Calculate CTh at each cortical point using the t_{link} metric ²⁶ and blur each subject's CTh map using a 20-millimeter full width at half maximum surface-based diffusion smoothing kernel (a necessary step to impose a normal distribution to corticometric data and to increase signal-to-noise ratio) ³⁷.

2.4 Visual Quality Control

Given the sensitivity of automated CTh measurements to small movement artefacts²⁵, a visual quality control (QC) of each subject's extracted white and gray matter surfaces was carried out by two independent investigators to ensure that there were no aberrations for a given subject (inter-rater reliability was .93) ³⁸ that could affect CTh estimates. Absolute CTh measures were also reviewed as extreme values (both very thin or very thick) can provide cues of poor surface recognition. The investigators were blinded with regards to age, gender, and other clinical variables. Table 1 provides a summary of reasons for QC failure. This QC procedure excluded MRI scans from: (1) subjects with the 2-D fallback protocols, who could not remain in the scanner for an extended period of time and had to undergo faster MRI image acquisition, resulting in a degree of resolution too low for an adequate estimation of CTh, (2) subjects with motion abnormalities resulting in an image processing failure, (3) subjects with strong field inhomogeneity in the image that could not be adequately corrected. Of note, this post-processing QC is a distinct process from the simple elimination of poor quality native MRI scans performed prior to applying the image-processing pipeline.

In total, 753 out of 954 MRI scans (410 females, 343 males) were kept for statistical analyses. This included 384 different subjects from ages 4.9 to 22.3 (age at the last follow-up scan) (mean 12.48 ± 3.9). 101 subjects had three MRI scans, 167 had two MRI scans and 116 had one MRI scan. Figure 1 shows the age distribution of all data points.

2.5 Statistical Analyses

Statistical analyses on vertex-wide CTh were implemented using SurfStat (<http://www.math.mcgill.ca/keith/surfstat/>), a statistical toolbox created for MATLAB (The MathWorks, Inc., Nathan, Massachusetts). Each subject's absolute native-space local CTh was linearly regressed against age in years (age in days/365.25) at each cortical point using mixed-effects models (diagonal structure). Mixed-effect models permit the implementation of linear regressions in samples combining subjects with different number of measurements, providing a way in which to analyze unbalanced longitudinal data while maximizing statistical power^{39–41}. In each mixed-effects model, subject ID was entered as a random effect in order to account for within-individual factors. Whole brain random field theory (RFT) $p < 0.05$ corrections (peaks and clusters) for multiple comparisons were applied for all statistical analyses. The age variable was mean centered for all analyses. To avoid confounding factors coming from the multisite nature of this study, scanner number was added as a categorical control variable in the models. There were significant differences in mean age between scanners (12 in total) because recent machines were only used for follow-up visits in which children were older. However, there was no 'scanner by age' interaction on mean cortical thickness (ANOVA $F(11,741)=0.677$; $p=0.761$). To facilitate comparison with other studies, terminology from the Desikan surface atlas was used to describe anatomical location of findings in this manuscript⁴².

In order to determine the best-fit model for the developmental trajectory of CTh, the most complex cubic model was tested first:

$$Y = \text{intercept} + b_1 \text{Sex} + b_2 \text{Scanner} + b_3 \text{Age} + b_4 \text{Age}^2 + b_5 \text{Age}^3 + \text{random}(\text{Subject_ID}) + \text{error}$$

In a second step, a quadratic model of development was tested to evaluate vertices that did not show a statistically significant cubic trajectory:

$$Y = \text{intercept} + b_1 \text{Sex} + b_2 \text{Scanner} + b_3 \text{Age} + b_4 \text{Age}^2 + \text{random}(\text{Subject_ID}) + \text{error}$$

In a third step, a first-order linear regression was implemented to evaluate brain areas that were not significant in cubic or quadratic models:

$$Y = \text{intercept} + b_1 \text{Sex} + b_2 \text{Scanner} + b_3 \text{Age} + \text{random}(\text{Subject_ID}) + \text{error}$$

It is well known that there is significant remodeling within the developing brain with different changes in cortical, subcortical, white matter and gray matter²³. To account for these relative changes, the above-described analyses were repeated adding total brain volume (TBV) as a covariate in the model. Of note, there is a monotonic relationship between TBV and mean CTh in our sample.

To determine if sex has an impact on CTh maturation, the 'age by sex' interaction was analyzed for all areas according to the previously identified best-fit trajectory (e.g., the age² by sex interaction was tested in an area if the best fit model was quadratic). TBV was

included as a control variable in all analyses involving sex comparisons to avoid having differences in brain size between sexes acting as a confounding factor²³.

To allow better comparison with data from other groups, scatterplots of mean CTh over time were produced. Statistical analyses of mean CTh were run using mixed-effects models (with AR(1) covariance structure) in SPSS version 19.0 (IBM Corporation, Armonk, New York), controlling for sex and scanner (all other vertex-wide analyses were done in SurfStat). The Akaike's Information Criterion was used to determine the optimal CTh trajectory model (first-order linear, quadratic, or cubic) factoring the goodness of fit and tradeoff of increasing the complexity of the model by adding terms. Similar analyses were conducted divided by the four main brain lobes.

2.6 Post-hoc Analyses - Impact of Quality Control Procedures

In order to verify the possible impact of QC on developmental trajectories, we reviewed CTh analyses at different levels of QC: 1) no QC (n=954), 2) the standard QC used in this study (n=753), 3) a very stringent QC eliminating subjects with even small areas of poorer definition (n=598). Table 1 provides criteria for the two QC levels and Figure 2 shows examples of the different reasons for failure (corresponding raw images can be found in supplementary material Figure A1). The sample without QC included subjects that could not tolerate the optimal scanning protocol and who were scanned with the 2D fall-back MR protocol (none of which passed the standard QC). A table providing the composition of the 3 samples can be found in the supplementary material (Table A1). Subjects who failed the QC were in average younger and had a higher proportion of males. The sample with no QC had a lower mean age and higher density of scans per subjects (i.e., more subjects with 2- or 3-scans) compared to the standard n=754 sample.

3. RESULTS

3.1 Cortical Thickness

As seen in figure 3, absolute CTh (i.e. results of analyses without including TBV) predominantly followed a first-order linear thinning trajectory. There were few areas showing cubic trajectories, such as the bilateral superior and inferior parietal cortex, left angular gyrus, left postero-lateral temporal cortex, left precentral gyrus, right dorsolateral prefrontal cortex (DLPFC) (superior frontal and rostral middle frontal areas), and left medial paracentral/superior frontal cortex. There were minimal areas demonstrating a quadratic fit in the periphery of cubic clusters. The remainder of the brain surface showed a progressive first-order linear decline over time, with only parts of the bilateral entorhinal cortices and medial temporal pole exhibiting no significant change over time.

As illustrated in figure 4, in the few areas where a cubic pattern was demonstrated, peaks of CTh were observed at, or prior to, age 8. In quadratic clusters, there was an acceleration of thinning over time with the peak at the beginning of the age sample (i.e., around age 5).

In terms of relative remodeling of the cortical mantle over time (i.e. when controlling for TBV) CTh followed an even more diffuse pattern of first-order linear decline (Figure 5).

Areas with cubic trajectories were more anatomically restricted compared to the analyses without TBV. Of note, there were no prefrontal regions showing a cubic best-fit.

3.2 Sex

Although males had thicker absolute cortices in multiple areas (figure 6 – part A), this difference was not significant when controlling for TBV. This means that gender does not have a specific effect on thickness beyond the global impact of male sex on overall brain size (i.e., a boy and a girl of the same age with the same brain size would have similar thickness on average). There were no statistically significant interactions between sex and local CTh in areas in which the developmental trajectory was either quadratic or cubic, suggesting that there are no sex differences in the age of CTh peaks within the age range of our sample. In areas best described by a first-order linear model, there was a significant gender interaction only in bilateral lateral occipital lobes (figure 6 – part B). As illustrated by the scatterplot in the Inline supplementary figure S1, males have faster thinning over time in this area.

3.3 Mean Cortical Thickness

For mean CTh across the whole brain, the first-order linear model was the most optimal model based on the Akaike's information criterion (first-level AIC -1057; quadratic AIC -1044; cubic AIC -1035). Results were similar when looking at the Bayesian criterion. Figure 7 shows the scatterplot of mean thickness across development and the breakdown by gender. The average thinning was 0.027mm per year. Boys had 1.9% thicker mean CTh than girls (males 3.611mm; females 3.544mm; $p < 0.001$), but both sexes had similar maturational trajectories. When controlling for TBV, thereby accounting for the average 10% volume difference between sexes, there was no significant difference in CTh between sexes (figure 7). Repeated analyses separated by brain lobes (right frontal, left frontal, right parietal, left parietal, right temporal, left temporal, right occipital, left occipital) demonstrated that the first-order model was the best fit in all lobes (Inline supplementary Figure S2).

3.4 Impact of Quality Control

As illustrated in figure 8, there was a shift toward a marked increase in the amount of areas with more complex trajectories when analyzing the sample without any QC ($n=954$) compared to the standard QC described above (69% more quadratic and cubic vertices) (Figure 8a and 8b). To ensure that the difference between the quantity of areas with quadratic/cubic trajectories between the no QC and QC'd analyses were not solely the result of a loss of power, we created a sample of 753 subjects from the no QC group by eliminating 201 subjects that were matched in terms of age and gender to the 201 subjects that have failed the QC. Analyses with this sample showed 30% more areas following a cubic/quadratic trajectory than the complete no QC sample (Inline supplemental material Figure S3). This strongly supports the view that the loss of quadratic/cubic areas with the standard QC is not simply due to loss of sample size, but is rather due to poorer quality images not being included in analyses. In fact, when directly contrasting CTh in the 201 subjects who failed the standard QC to an age and gender matched group of 201 scans that passed the QC, the failed scans showed statistically significant thinner cortex diffusely (Inline supplementary material Figure S4). Interestingly, in the subsample of subjects that

passed the more stringent QC (n=598), thereby including only the best quality data, there were almost no areas (1.4% of the total brain surface) showing quadratic or cubic trajectories (Figure 8c).

4. DISCUSSION

This study revisited developmental trajectories of CTh in the longitudinal sample of the NIH MRI Study of Normal Brain development, which is socio-demographically representative of the American population. A few key findings emerged. First, we found that CTh predominantly follows a monotonic first-order linear decline over time between the age of 4.9 and 22.3, in line with multiple other studies^{15–18}. There were few areas showing cubic trajectories. Some of these regions are in line with other studies finding later peaks in association areas, including bilateral posterior parietal areas, posterior temporo-parietal areas, and right DLPFC^{3,20}. However, we also found a cubic trajectory in the left motor/premotor strip. When controlling for total brain volume, most of the cortex followed a first-order linear decline over time, including the entire frontal lobes. Of note, within the few areas of cubic trajectories, all CTh peaks were at, or prior to age 8, which is an earlier peak than previously reported in other studies^{3,14}. Results for CSA provided in the associated Data in Brief article²⁴ showed that the great majority of the brain's surface did not change over time within the age range of this sample, especially when controlling for TBV. In terms of CV,²⁴ when controlling for TBV, most of the cortical mantle followed a monotonic linear decline reflecting the impact of CTh changes. Notable exceptions included bilateral medial temporal areas, temporal poles, and the ACC, which showed no change over time. For the ACC the absence of change represents the combination of cortical thinning with concurrent expansion of CSA.

In addition, the only sex difference in CTh maturation involved restricted regions of the lateral occipital lobe bilaterally. Faster thinning in the occipital lobe of boys was also reported by another group²⁰, but the impacts of sex was much more anatomically restricted in our results. We did not identify any sex differences in the age of CTh peaks within this age range, in contrast to some^{8,20,43}, but not all^{14,18} previous reports. In light of our results, controlling for total brain volume (or another measure of global brain size) when comparing genders in terms of brain-behavior relationships should be considered to avoid the confounding effect of the baseline 10% brain size difference between sexes.²³ However, the decision to include or not a control for total brain volume has to be decided based on the specific research question, as the biological meaning of analyzing the residual impact of sex beyond the difference in total brain size is uncertain.

The gradual thinning of the cortex is a normative phenomenon reflecting the progressive maturation of brain organization. The biological underpinnings of variations in developmental trajectories cannot be extrapolated from correlational neuroimaging studies. However, data from histological studies suggest that age-related CTh trajectories are the result of a combination of competing changes⁴⁴. For instance, while the number of brain synapses peaks at around 3 years of age, there is still ongoing development of dendrites in childhood⁴⁵. Rates of synaptic formation and ongoing dendritic development (and associated glial support) may vary as a function of cortical region. In parallel, neocortical

myelination in humans is known to start in infancy and extend into young adulthood⁴⁶. It is important to keep in mind that MRI-based estimates of CTh may also partly be influenced by the progressive myelination of intra-cortical fibers, which could change the MRI signal in lower layers of the cortex, contributing to the progressive decline in MRI-based CTh estimation with aging⁴⁶⁻⁴⁸. A gradual synaptic pruning of inefficient connections in childhood and adolescence could lead to a decrease in gray matter thickness^{49,50}. Changes in neuronal size, glial cell density, and vasculature could also contribute to CTh changes⁵¹. Finally, a recent study suggested that cortical thinning and gyral white matter expansion in adolescence parallel increased sulcal widening and reduced sulcal depth, described as a 'flattening' of the cerebral cortex⁵². In terms of the reason why quadratic and cubic curves peak later in some brain areas, previous studies have suggested a link between the complexity of laminar cortical architecture and the complexity of developmental trajectories³. The isocortex of associative areas was hypothesized to have a more prolonged development than phylogenically older areas (allocortex). The areas identified as having quadratic/cubic trajectories in our sample were indeed part of this isocortex, however it remains unexplained why these areas showed later cortical thickness peaks than other brain regions within the isocortex.

The cortical maturation trajectories observed in our results differ from previous reports of an inverted U-shape development of gray matter^{3,12,13}. Other than differences in sample composition and the multi-site nature of this study, several factors could explain this discrepancy. First, initial studies mainly looked at cortical volume, which is different than the CTh metric used here. Second, automated cortical morphometric pipelines have improved over the years. A significant change has been the introduction of iterative hemisphere-specific template registration algorithms, which have improved the reliability of CTh measurements. Third, the Shaw et al. (2008) study included a sample with a wider age range (3.5 to 33). Since the sample in this study stopped at 22.3 years of age, this could have limited the capacity to identify a phase of stabilization in cortical thinning in the late 20s. It is plausible that CTh may follow a cubic pattern of development in humans, however our results imply that peaks of CTh have to occur at an earlier age (i.e. around 5 years of age) than previously reported in most brain areas.

Our results on the impact of QC on the estimations of cortical trajectories demonstrate that part of the discrepancy between groups could be related to methodology. Indeed, there was a clear shift toward increased areas with more complex trajectories (quadratic and cubic) when no QC was implemented. In addition, in the stringent QC sample including only the best quality data there were almost no areas with complex trajectories. Since this sample was large enough (n=595) to have the statistical power to detect the strong impact of age on CTh over time, we argue that this further supports the notion that CTh developmental trajectories follow mostly a first-order linear decline trajectory between 4.9 and 22.3 years of age.

In our sample, subjects who failed the standard QC had lower CTh than age and gender matched subjects who passed the QC. This is in line with a recent study demonstrating that movement artifacts lead to an underestimation of CTh²⁵. Young children tend to be overrepresented in QC failure due to a higher tendency to move during scanning. Logically, if failed automated processing yields underestimations of CTh, and young subjects have

poorer imaging quality, this could artificially create quadratic/cubic trajectories. In light of these results, we argue that researchers should be careful to implement an equivalent to the standard degree of QC (which should be described in manuscript) in studies involving children and clinical populations in order to obtain valid results that are more likely to be replicable and translatable in clinical practice. It is crucial that the QC process includes a post-processing component, as the visual review of raw images is not sufficient to identify subtle movement artifacts. While the relatively high rate of failure observed with our QC can work in large dataset, it becomes more problematic in smaller data sets. One factor to consider is that this study included young children who tend to move more than adults during scanning; therefore a lower failure rate would be expected in adults. In our experience, the loss in power from losing subjects is compensated by minimizing artificially inflated variance caused by movement artifacts.

5. CONCLUSIONS

In summary, CTh follows a negative first-order linear trajectory in most of the brain between the ages of 4.9 and 22, with a mean decline of 0.027 mm per year. In areas of cubic trajectories, peaks of CTh occurred no later than at 8 years of age. The only sexually dimorphic finding was faster thinning in parts of the occipital lobe of boys compared to girls. Crucially, the application of a visual QC to ensure the reliability of data shifts identified trajectories from more complex models to a first-order linear one. The rate of cortical thinning was found to be associated with the development of neuropsychiatric disorders^{10,53} and could constitute a potential biomarker for disease states. Based on these results, it will be crucial in future studies to implement postprocessing pipeline output QC to avoid spurious findings resulting from inadequate estimations of CTh related to movement and other artifacts.

Supplementary Material

Refer to Web version on PubMed Central for supplementary material.

Acknowledgments

This project has been funded in whole or in part with Federal funds from the National Institute of Child Health and Human Development, the National Institute on Drug Abuse, the National Institute of Mental Health, and the National Institute of Neurological Disorders and Stroke (Contract #s N01-HD02-3343, N01-MH9-0002, and N01-NS-9-2314, -2315, -2316, -2317, -2319 and -2320). SD receives funding from the Montreal General Hospital Foundation, the Montreal Neurological Institute and the *Fonds de Recherche du Québec-Santé*. SK and AL receive funding from the *Fonds de Recherche du Québec-Santé*. ACE receives funding from the Canadian Institutes of Health Research, Brain Canada, and the National Institutes of Health. Authors want to acknowledge The Azrieli Neurodevelopmental Research Program and the Canadian Institutes for Health Research for supporting the analytic capabilities required for this work.

Abbreviations

CSA	Cortical surface area
CTh	Cortical thickness
CV	Cortical volume

DLPFC	Dorsolateral prefrontal cortex
MRI	magnetic resonance imaging
QC	Quality control
RFT	Random field theory
TBV	Total brain volume

References

1. Clouchoux C, Guizard N, Evans A, du Plessis A, Limperopoulos C. Normative fetal brain growth by quantitative in vivo magnetic resonance imaging. *Am J Obstet Gynecol.* 2012; 206(173):e1–e8. [PubMed: 22055336]
2. Giedd J, Rapoport J. Structural MRI of pediatric brain development: what have we learned and where are we going? *Neuron.* 2010; 67:728–734. [PubMed: 20826305]
3. Shaw P, Kabani N, Lerch J, et al. Neurodevelopmental trajectories of the human cerebral cortex. *J Neurosci.* 2008; 28(14):3586–3594. [PubMed: 18385317]
4. Giedd J, Lalonde F, Celano M, et al. Anatomical brain magnetic resonance imaging of typically developing children and adolescents. *J Am Acad Child Adolesc Psychiatry.* 2009; 48(5):465–470. [PubMed: 19395901]
5. Shaw P, Gilliam M, Liverpool M, et al. Cortical development in typically developing children with symptoms of hyperactivity and impulsivity: support for a dimensional view of attention deficit hyperactivity disorder. *Am J Psychiatry.* 2011; 168:143–151. [PubMed: 21159727]
6. Ducharme S, Hudziak J, Botteron K, et al. Decreased regional cortical thickness and thinning rate are associated with inattention symptoms in healthy children. *J Am Acad Child Adolesc Psychiatry.* 2012; 51(1):18–27. [PubMed: 22176936]
7. Shaw P, Greenstein D, Lerch J, et al. Intellectual ability and cortical thickness development in children and adolescents. *Nature.* 2006; 440:676–679. [PubMed: 16572172]
8. Lenroot R, Gogtay N, Greenstein D, et al. Sexual dimorphism of brain development trajectories during childhood and adolescence. *NeuroImage.* 2007; 36:1065–1073. [PubMed: 17513132]
9. Kharitonova M, Martin RE, Gabrieli JD, Sheridan MA. Cortical gray-matter thinning is associated with age-related improvements on executive function tasks. *Dev Cogn Neurosci.* Oct.2013 6:61–71. [PubMed: 23896579]
10. Thormodsen R, Rimol LM, Tamnes CK, et al. Age-related cortical thickness differences in adolescents with early-onset schizophrenia compared with healthy adolescents. *Psychiatry Res.* Dec 30; 2013 214(3):190–196. [PubMed: 24144503]
11. Ducharme S, Albaugh MD, Hudziak JJ, et al. Anxious/depressed symptoms are linked to right ventromedial prefrontal cortical thickness maturation in healthy children and young adults. *Cereb Cortex.* 2013:bht151.
12. Giedd J, Blumenthal J, Jeffries N, et al. Brain development during childhood and adolescence: a longitudinal MRI study. *Nat Neurosci.* 1999; 2(10):861–863. [PubMed: 10491603]
13. Gogtay N, Giedd J, Lusk L, et al. Dynamic mapping of human cortical development during childhood through early adulthood. *Proc Natl Acad Sci USA.* 2004; 101(21):8174–8179. [PubMed: 15148381]
14. Raznahan A, Shaw P, Lalonde F, et al. How does your cortex grow? *J Neurosci.* 2011; 31(19): 7174–7177. [PubMed: 21562281]
15. Sowell E, Thompson P, Leonard C, Welcome S, Kan E, Toga A. Longitudinal mapping of cortical thickness and brain growth in normal children. *J Neurosci.* 2004; 24(38):8223–8231. [PubMed: 15385605]
16. Muftuler L, Davis E, Buss C, Head K, Hasso A, Sandman C. Cortical and subcortical changes in typically developing preadolescent children. *Brain Research.* 2011; 1399:15–24. [PubMed: 21640983]

17. Tamnes CK, Østby Y, Fjell AM, Westlye LT, Due-Tønnessen P, Walhovd KB. Brain maturation in adolescence and young adulthood: regional age-related changes in cortical thickness and white matter volume and microstructure. *Cereb Cortex*. 2010; 20(3):534–548. [PubMed: 19520764]
18. Cédric P, Koolschijn M, Crone EA. Sex differences and structural brain maturation from childhood to early adulthood. *Developmental Cognitive Neuroscience*. 2013
19. van Soelen I, Brouwer R, van Baal G, et al. Genetics influences on thinning of the cerebral cortex during development. *NeuroImage*. 2012; 59:3871–3880. [PubMed: 22155028]
20. Mutlu AK, Schneider M, Debbané M, Badoud D, Eliez S, Schaer M. Sex differences in thickness, and folding developments throughout the cortex. *NeuroImage*. Nov 15.2013 82:200–207. [PubMed: 23721724]
21. Evans A. Brain Development Cooperative Group. The NIH MRI study of normal brain development. *NeuroImage*. 2006; 30:184–202. [PubMed: 16376577]
22. Waber D, De Moor C, Forbes P, et al. The NIH MRI study of normal brain development: Performance of a population based sample of healthy children aged 6 to 18 years on a neuropsychological battery. *Journal of the International Neuropsychological Society*. 2007; 13(5): 729–746. [PubMed: 17511896]
23. Brain Development Cooperative Group. Total and regional brain volumes in a population-based normative sample from 4 to 18 years: The NIH MRI Study of Normal Brain Development. *Cereb Cortex*. 2012; 22:1–12. [PubMed: 21613470]
24. Ducharme S, Albaugh M, Nguyen T, et al. Trajectories of cortical surface area and cortical volume maturation in normal brain development. *Data in Brief*. 2015 In Press.
25. Reuter M, Tisdall MD, Qureshi A, Buckner RL, van der Kouwe AJ, Fischl B. Head motion during MRI acquisition reduces gray matter volume and thickness estimates. *NeuroImage*. Dec 10.2014 107c:107–115. [PubMed: 25498430]
26. Lerch JP, Evans AC. Cortical thickness analysis examined through power analysis and a population simulation. *NeuroImage*. Jan 1; 2005 24(1):163–173. [PubMed: 15588607]
27. Kabani N, Le Goualher G, MacDonald D, Evans AC. Measurement of cortical thickness using an automated 3-D algorithm: a validation study. *NeuroImage*. Feb; 2001 13(2):375–380. [PubMed: 11162277]
28. Talairach, J.; Tournoux, P. Co-planar stereotaxic atlas of the human brain: 3-dimensional proportional system: an approach to cerebral imaging. Stuttgart; New York: G. Thieme; New York: Thieme Medical Publishers; 1988.
29. Collins DL, Neelin P, Peters TM, Evans AC. Automatic 3D intersubject registration of MR volumetric data in standardized Talairach space. *Journal of computer assisted tomography*. Mar-Apr;1994 18(2):192–205. [PubMed: 8126267]
30. Mazziotta JC, Toga AW, Evans A, Fox P, Lancaster J. A probabilistic atlas of the human brain: theory and rationale for its development. *The International Consortium for Brain Mapping (ICBM)*. *NeuroImage*. Jun; 1995 2(2):89–101. [PubMed: 9343592]
31. Sled JG, Zijdenbos AP, Evans AC. A nonparametric method for automatic correction of intensity nonuniformity in MRI data. *IEEE transactions on medical imaging*. Feb; 1998 17(1):87–97. [PubMed: 9617910]
32. Zijdenbos AP, Forghani R, Evans AC. Automatic “Pipeline” Analysis of 3-D MRI Data for Clinical Trials: Application to Multiple Sclerosis. *IEEE transactions on medical imaging*. 2002; 21:1280–1291. [PubMed: 12585710]
33. Kim JS, Singh V, Lee JK, et al. Automated 3-D extraction and evaluation of the inner and outer cortical surfaces using a Laplacian map and partial volume effect classification. *NeuroImage*. Aug 1; 2005 27(1):210–221. [PubMed: 15896981]
34. MacDonald D, Kabani N, Avis D, Evans AC. Automated 3-D extraction of inner and outer surfaces of cerebral cortex from MRI. *NeuroImage*. Sep; 2000 12(3):340–356. [PubMed: 10944416]
35. Lyttelton O, Boucher M, Robbins S, Evans A. An unbiased iterative group registration template for cortical surface analysis. *NeuroImage*. Feb 15; 2007 34(4):1535–1544. [PubMed: 17188895]

36. Grabner G, Janke AL, Budge MM, Smith D, Pruessner J, Collins DL. Symmetric atlas and model based segmentation: an application to the hippocampus in older adults. *Med Image Comput Assist Interv Int Conf Med Image Comput Assist Interv*. 2006; 9(Pt 2):58–66.
37. Chung MK, Worsley KJ, Taylor J, Ramsay JO, Robbins S, Evans AC. Diffusion Smoothing on the Cortical Surface. *NeuroImage*. 2001; 13S:95.
38. Karama S, Ad-Dab'bagh Y, Haier RJ, et al. Positive association between cognitive ability and cortical thickness in a representative US sample of healthy 6 to 18 year-olds (vol 37, pg 145, 2009). *Intelligence*. Jul-Aug;2009 37(4):431–442.
39. Diggle, P. *Analysis of longitudinal data*. 2. Oxford; New York: Oxford University Press; 2002.
40. Shaw P, Gilliam M, Liverpool M, et al. Cortical development in typically developing children with symptoms of hyperactivity and impulsivity: support for a dimensional view of attention deficit hyperactivity disorder. *Am J Psychiatry*. Feb; 2011 168(2):143–151. [PubMed: 21159727]
41. Singer, JD.; Willett, JB. *Applied longitudinal data analysis: modeling change and event occurrence*. Oxford; New York: Oxford University Press; 2003.
42. Desikan RS, Ségonne F, Fischl B, et al. An automated labeling system for subdividing the human cerebral cortex on MRI scans into gyral based regions of interest. *NeuroImage*. 2006; 31(3):968–980. [PubMed: 16530430]
43. Giedd J, Blumenthal J, Jeffries N, et al. Brain development during childhood and adolescence: a longitudinal MRI study. *Nature Neuroscience*. 1999; 2(10):861–863. [PubMed: 10491603]
44. Kostovic I, Jovanov-Milosevic N, Rados M, et al. Perinatal and early postnatal reorganization of the subplate and related cellular compartments in the human cerebral wall as revealed by histological and MRI approaches. *Brain Struct Funct*. Jan; 2014 219(1):231–253. [PubMed: 23250390]
45. Petanjek Z, Judas M, Kostovic I, Uylings HB. Lifespan alterations of basal dendritic trees of pyramidal neurons in the human prefrontal cortex: a layer-specific pattern. *Cereb Cortex*. Apr; 2008 18(4):915–929. [PubMed: 17652464]
46. Miller DJ, Duka T, Stimpson CD, et al. Prolonged myelination in human neocortical evolution. *Proc Natl Acad Sci USA*. Sep 24.2012 109:16480–16485. [PubMed: 23012402]
47. Paus T, Keshavan M, Giedd JN. Why do many psychiatric disorders emerge during adolescence? *Nature Reviews Neuroscience*. 2008; 9(12):947–957. [PubMed: 19002191]
48. Glasser MF, Van Essen DC. Mapping human cortical areas in vivo based on myelin content as revealed by T1- and T2-weighted MRI. *J Neurosci*. 2011; 31(32):11597–11616. [PubMed: 21832190]
49. Bourgeois J-P, Goldman-Rakic PS, Rakic P. Synaptogenesis in the Prefrontal Cortex of Rhesus Monkeys. *Cereb Cortex*. Jan 1; 1994 4(1):78–96. [PubMed: 8180493]
50. Huttenlocher PR. Morphometric study of human cerebral cortex development. *Neuropsychologia*. 1990; 28(6):517–527. [PubMed: 2203993]
51. Zatorre RJ, Fields RD, Johansen-Berg H. Plasticity in gray and white: neuroimaging changes in brain structure during learning. *Nature Neuroscience*. 2012; 15(4):528–536. [PubMed: 22426254]
52. Aleman-Gomez Y, Janssen J, Schnack H, et al. The human cerebral cortex flattens during adolescence. *J Neurosci*. Sep 18; 2013 33(38):15004–15010. [PubMed: 24048830]
53. Shaw P, Eckstrand K, Sharp W, et al. Attention-deficit/hyperactivity disorder is characterized by a delay in cortical maturation. *Proc Natl Acad Sci USA*. 2007; 104(49):19649–19654. [PubMed: 18024590]

Brain Development Cooperative Group

Key personnel from the six pediatric study centers are as follows: **Children's Hospital Medical Center of Cincinnati**, Principal Investigator William S. Ball, M.D., Investigators Anna Weber Byars, Ph.D., Mark Schapiro, M.D., Wendy Bommer, R.N., April Carr, B.S., April German, B.A., Scott Dunn, R.T.; **Children's Hospital Boston**, Principal Investigator Michael J. Rivkin, M.D., Investigators Deborah Waber, Ph.D., Robert Mulkern, Ph.D.,

Sridhar Vajapeyam, Ph.D., Abigail Chiverton, B.A., Peter Davis, B.S., Julie Koo, B.S., Jacki Marmor, M.A., Christine Mrakotsky, Ph.D., M.A., Richard Robertson, M.D., Gloria McAnulty, Ph.D.; **University of Texas Health Science Center at Houston**, Principal Investigators Michael E. Brandt, Ph.D., Jack M. Fletcher, Ph.D., Larry A. Kramer, M.D., Investigators Grace Yang, M.Ed., Cara McCormack, B.S., Kathleen M. Hebert, M.A., Hilda Volero, M.D.; **Washington University in St. Louis**, Principal Investigators Kelly Botteron, M.D., Robert C. McKinstry, M.D., Ph.D., Investigators William Warren, Tomoyuki Nishino, M.S., C. Robert Almlı, Ph.D., Richard Todd, Ph.D., M.D., John Constantino, M.D.; **University of California Los Angeles**, Principal Investigator James T. McCracken, M.D., Investigators Jennifer Levitt, M.D., Jeffrey Alger, Ph.D., Joseph O’Neil, Ph.D., Arthur Toga, Ph.D., Robert Asarnow, Ph.D., David Fadale, B.A., Laura Heinichen, B.A., Cedric Ireland B.A.; **Children’s Hospital of Philadelphia**, Principal Investigators Dah-Jyuu Wang, Ph.D. and Edward Moss, Ph.D., Investigators Robert A. Zimmerman, M.D., and Research Staff Brooke Bintliff, B.S., Ruth Bradford, Janice Newman, M.B.A. The Principal Investigator of the data coordinating center at **McGill University** is Alan C. Evans, Ph.D., Investigators Rozalia Arnaoutelis, B.S., G. Bruce Pike, Ph.D., D. Louis Collins, Ph.D., Gabriel Leonard, Ph.D., Tomas Paus, M.D., Alex Zijdenbos, Ph.D., and Research Staff Samir Das, B.S., Vladimir Fonov, Ph.D., Luke Fu, B.S., Jonathan Harlap, Ilana Leppert, B.E., Denise Milovan, M.A., Dario Vins, B.C., and at **Georgetown University**, Thomas Zeffiro, M.D., Ph.D. and John Van Meter, Ph.D. Ph.D. Investigators at the Neurostatistics Laboratory, **Harvard University/McLean Hospital**, Nicholas Lange, Sc.D., and Michael P. Froimowitz, M.S., work with data coordinating center staff and all other team members on biostatistical study design and data analyses. The Principal Investigator of the Clinical Coordinating Center at **Washington University** is Kelly Botteron, M.D., Investigators C. Robert Almlı Ph.D., Cheryl Rainey, B.S., Stan Henderson M.S., Tomoyuki Nishino, M.S., William Warren, Jennifer L. Edwards M.S.W., Diane Dubois R.N., Karla Smith, Tish Singer and Aaron A. Wilber, M.S. The Principal Investigator of the Diffusion Tensor Processing Center at the **National Institutes of Health** is **Carlo Pierpaoli, MD, Ph.D.**, Investigators **Peter J. Basser, Ph.D., Lin-Ching Chang, Sc.D.**, Chen Guan Koay, **Ph.D. and Lindsay Walker, M.S.** The Principal Collaborators at the **National Institutes of Health** are Lisa Freund, Ph.D. (NICHD), Judith Rumsey, Ph.D. (NIMH), Lauren Baskir, Ph.D. (NIMH), Laurence Stanford, Ph.D. (NIDA), Karen Sirocco, Ph.D. (NIDA) and from NINDS, Katrina Gwinn-Hardy, M.D., and Giovanna Spinella, M.D. The Principal Investigator of the Spectroscopy Processing Center at the **University of California Los Angeles** is **James T. McCracken, M.D.**, Investigators Jeffrey R. Alger, Ph.D., Jennifer Levitt, M.D., Joseph O’Neill, Ph.D.

Highlights

- Cortical thickness follows mostly a monotonic linear decline after 5 years of age
- Areas with cubic developmental trajectories have peaks of cortical thickness prior to age 8
- The only sex difference in maturation is faster occipital thinning in males
- Mean cortical thickness follows a monotonic decline of 0.027mm per year
- Quality control processes have a significant impact on identified trajectories
- A post-processing quality control should be applied in all cortical thickness studies

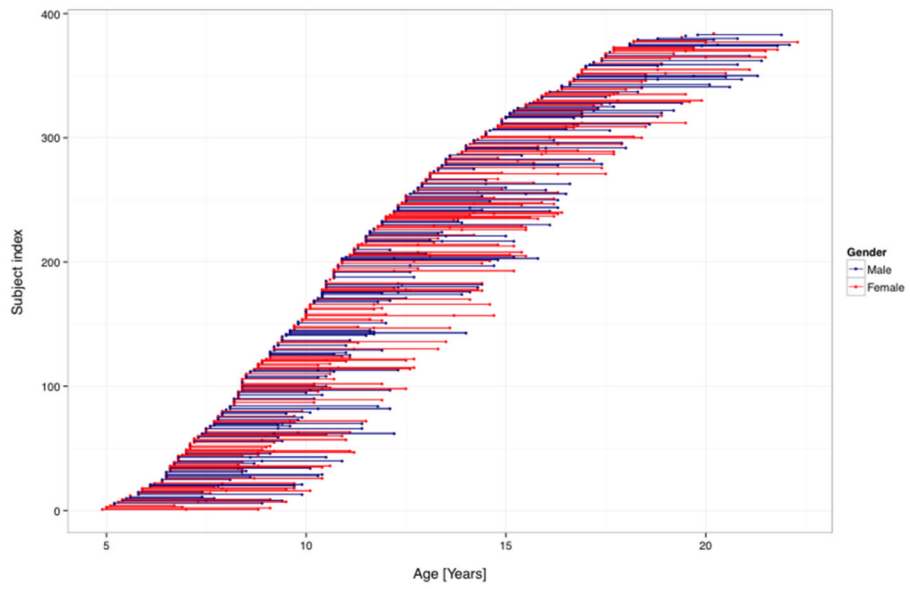


Figure 1. Age distribution of subjects including age at repeated scans. (n=384 subjects; 753 scans). Each dot represents a datapoint. Individual subjects are depicted by a dot (subject with one MRI) or a line (2 or 3 MRIs). Male subjects are in blue, female subjects in red.

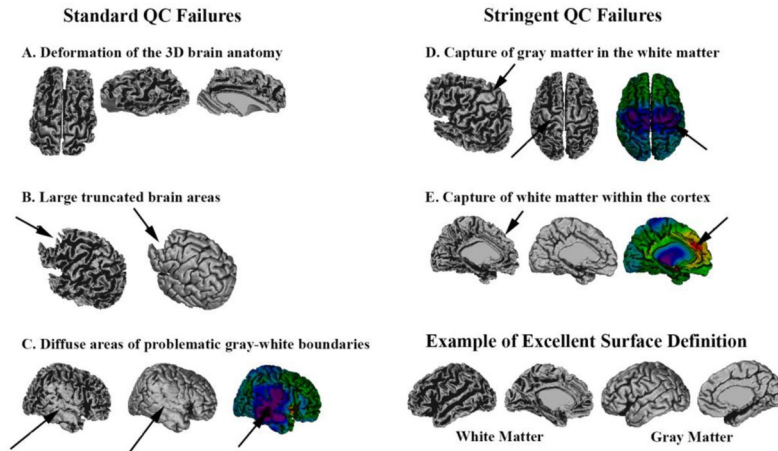


Figure 2.

This figure depicts examples of the different reasons why scans have failed the standard quality control (QC) (left column) or the stringent QC (right column). An example with excellent surface definition is provided for comparison (bottom right). Standard QC Failures: Image A is an example of gross deformation of the overall three-dimensional (3D) shape of the brain. Part B shows a more normal global structure, but with significant parts of the frontal lobes truncated. Image C demonstrates large areas of capture of gray matter in the white matter surface, leading to impaired gyrification and underestimated cortical thickness (blue-purple colors).

Stringent QC Failures: Part D demonstrates the capture of some gray matter within the white matter surface in the pericentral areas (an area with frequent grey-white boundaries problems), but the great majority of the surface is adequately defined. Figure E shows a poor definition of white matter folds in the dorsal medial frontal areas due the capture of some white matter in the cortex, which leads to increased cortical thickness estimations (yellow-red colors). Associated raw MRI images are provided in supplementary materiel (Figure A1)

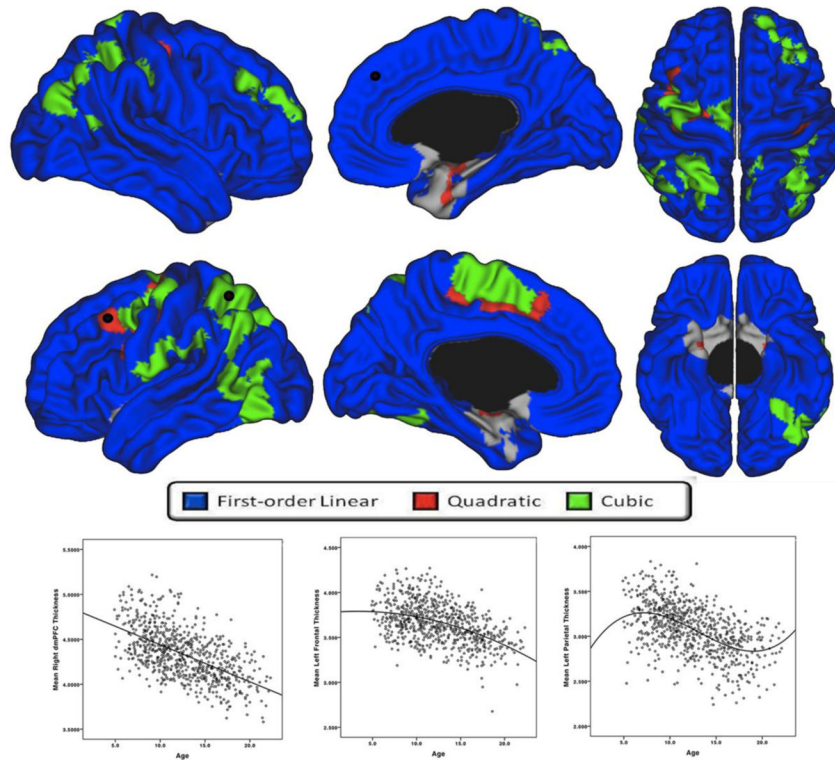


Figure 3. Developmental trajectories of absolute local cortical thickness (i.e., not controlled for total brain volume) from 4.9 to 22.3 years of age, controlling for sex and scanner (standard QC, n=753). Brain areas for which the best-fit model is cubic are in green, quadratic in red, and first-order linear in blue. Scatterplots of cortical thickness (mm) in representative brain areas (identified with black dot) demonstrating a significant cubic (left plot - left superior parietal cortex), quadratic (middle plot – left caudal middle frontal gyrus) and first-order linear (right plot -dorsomedial prefrontal cortex) trajectory are provided for visualization purpose.

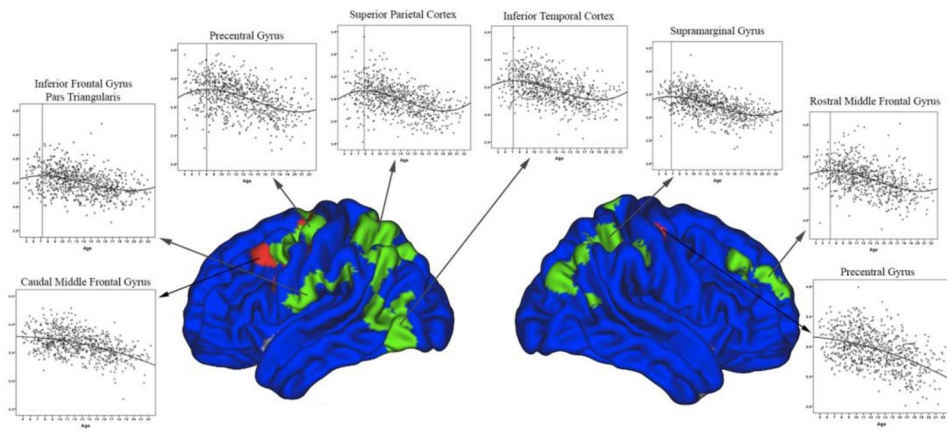


Figure 4. Scatterplots of cortical thickness in brain areas demonstrating significant quadratic and cubic trajectories over time. All cortical thickness peaks occurred at, or prior to, age 8.

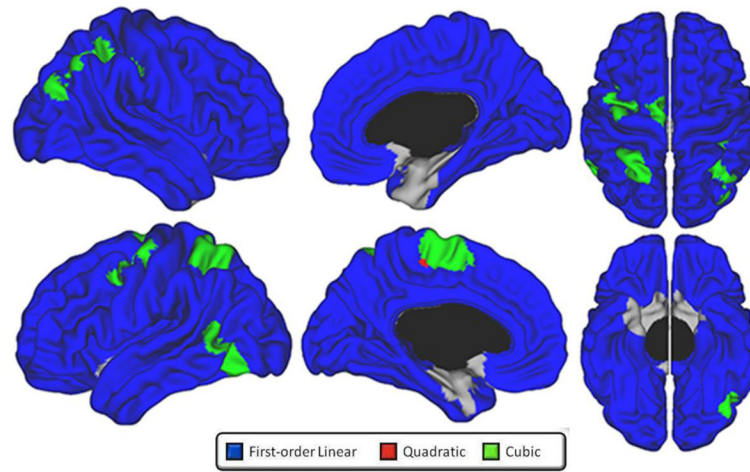
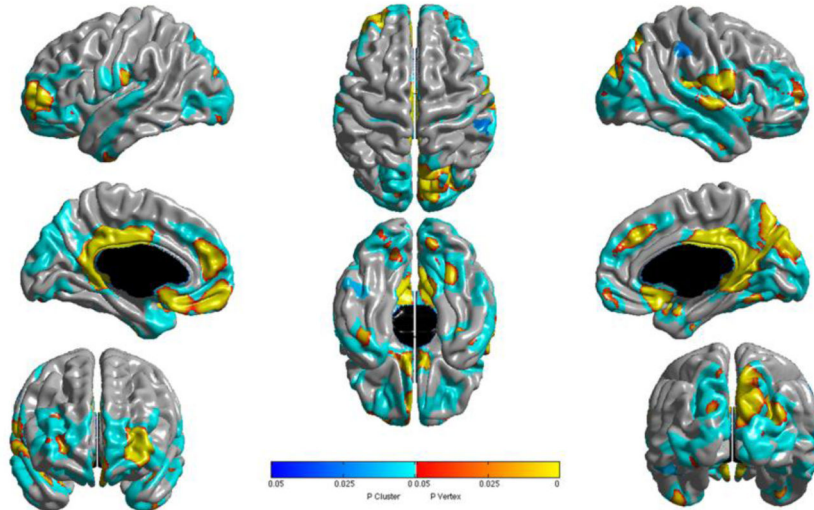


Figure 5. Developmental trajectories of local cortical thickness from 4.9 to 22.3 years of age, controlling for total brain volume, sex and scanner (standard QC, n=753). Brain areas for which the best-fit model is cubic are in green, quadratic in red, and first-order linear in blue.

A. Brain areas with thicker cortex in males compared to females



B. Brain areas showing an interaction between age and sex

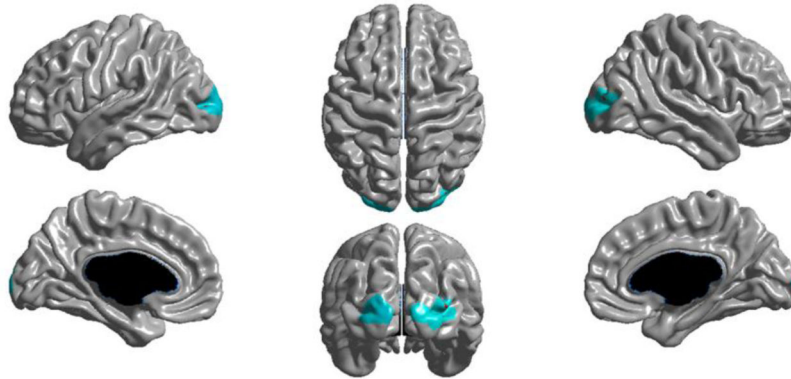


Figure 6.

A. Brain areas in which males show thicker absolute cortices than females controlling for age and scanner, but not for total brain volume. No areas were significant when controlling for total brain volume. B. Brains areas in which there is a significant age by sex interaction on cortical thickness, controlling for scanner and total brain volume. Areas in shades of red-yellow are significant at the vertex level, and areas in shades of blue at the cluster level (random field theory corrected).

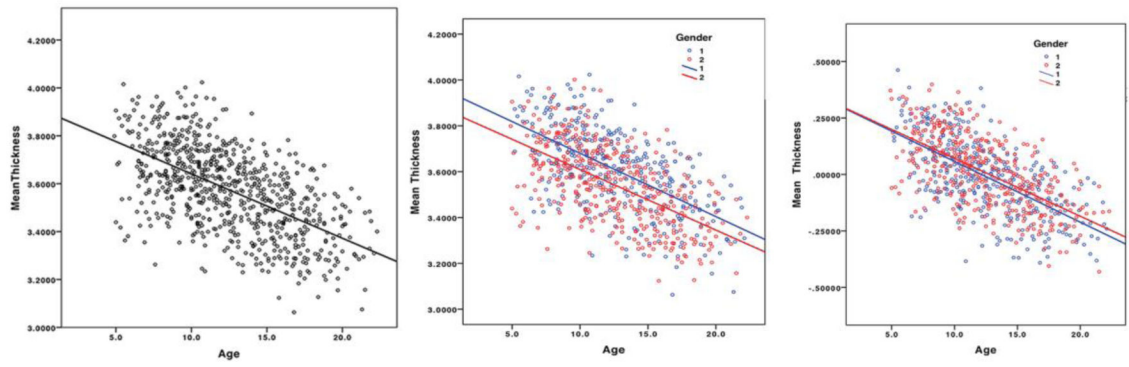


Figure 7. Mean cortical thickness across development. The left-hand side plot represents the complete sample with absolute mean thickness measures on the Y-axis. The middle plot depicts absolute values after sex partitioning, with males in blue (group 1), and females in red (group 2). The right-hand side graph shows mean CTh after controlling for total brain volume (unstandardized residuals), with gender partitioning.

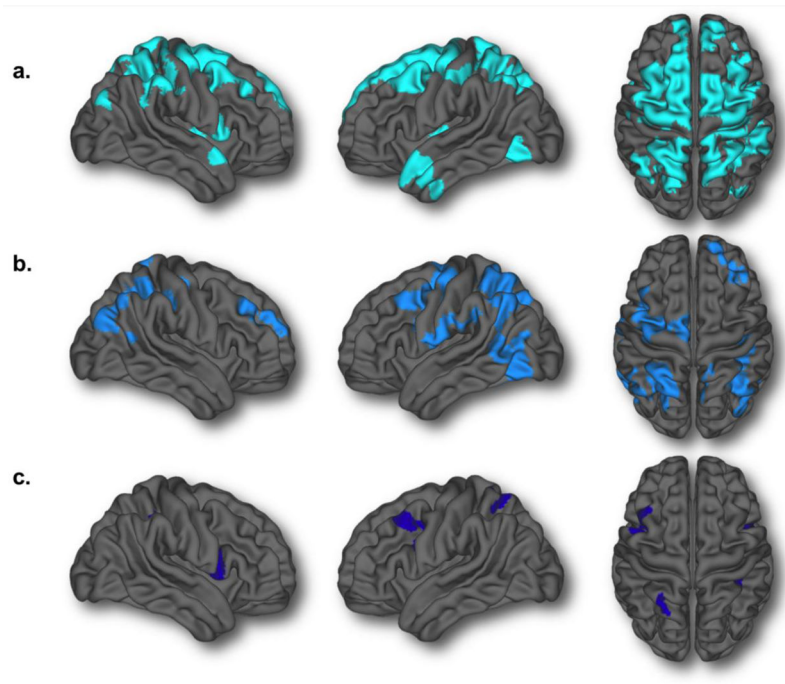


Figure 8.

Brain areas demonstrating either quadratic or cubic developmental trajectories at three levels of quality control: a) no quality control (n=954) [13,435 total vertices; 16.4% of the brain] b) standard quality control (used in the manuscript, n=753) [7,932 total vertices; 9.7% of the brain] c) stringent quality control (n=598) [1,133 vertices; 1.4% of the brain].

Table 1

Synoptic table of the reasons for quality control failures at two levels of severity

Quality Control Level	Reasons for Failure
Standard QC	Excludes all subjects with: <ul style="list-style-type: none"> a. Gross deformation of the three-dimensional brain anatomy b. Large truncated brain areas c. Diffuse areas of problematic gray-white boundaries definition
Stringent QC	Excludes all subjects with: <ul style="list-style-type: none"> a. Failure of the standard QC b. Localized areas of imprecise cortical definition <ul style="list-style-type: none"> • Inclusion of white matter within cortex • Capture of gray matter in the white matter

Author Manuscript

Author Manuscript

Author Manuscript

Author Manuscript